

Inert Extension of the Zee-Babu Model

Hiroshi Okada,^{1,*} Takashi Toma,^{2,†} and Kei Yagyu^{3,‡}

¹*School of Physics, KIAS, Seoul 130-722, Korea*

²*Institute for Particle Physics Phenomenology*

University of Durham, Durham DH1 3LE, United Kingdom

³*Department of Physics and Center for Mathematics and Theoretical Physics,*

National Central University, Chungli, Taiwan 32001, ROC

We propose a two-loop induced Zee-Babu type neutrino mass model at the TeV scale. Although there is no dark matter candidate in the original Zee-Babu model, that is contained in our model by introducing an unbroken discrete Z_2 symmetry. The discrepancy between the experimental value of the muon anomalous magnetic moment (muon $g - 2$) and its prediction in the standard model can be explained by contributions from additional vector-like charged-leptons which are necessary to give non-zero neutrino masses. The mass of vector-like leptons to be slightly above 300 GeV is favored and allowed from the muon $g - 2$ and the current LHC data. We find that from the structure of neutrino mass matrix, doubly-charged scalar bosons in our model can mainly decay into the same-sign and same-flavour dilepton plus missing transverse momentum. By measuring an excess of these events at the LHC, our model can be distinguished from the other models including doubly-charged scalar bosons.

PACS numbers:

*Electronic address: hokada@kias.re.kr

†Electronic address: takashi.toma@durham.ac.uk

‡Electronic address: keiyagyu@ncu.edu.tw

I. INTRODUCTION

From the discovery of the Higgs boson at the CERN Large Hadron Collider (LHC) [1, 2], our standard picture for the spontaneous breakdown of electroweak symmetry has been confirmed. This fact tells us that the standard model (SM) well describes phenomena at collider experiments even including the Higgs sector.

In spite of the great success of the SM, we need to consider new physics models beyond the SM, because there are phenomena which cannot be explained in the SM such as neutrino oscillations and the existence of dark matter (DM). Therefore, further new particles are expected to be found at the 13 and 14 TeV runs of the LHC, which can be a direct evidence of new physics models.

Radiative neutrino mass models give an attractive new physics scenario to explain tiny neutrino masses which are generated at loop levels. Because of loop suppression, masses of new particles can be taken at the TeV scale, so that radiative neutrino mass models may be able to directly tested at collider experiments. The Zee model [3] and the Zee-Babu model [4] have been proposed in 1980s, in which Majorana type masses are generated at the one loop and two loop levels, respectively. After these models appeared, the three-loop neutrino mass model has been constructed by Krauss, Nasri and Trodden [5] in the early 2000s, in which a right-handed neutrino running in the loop can be a DM candidate. In addition, the model by Ma [6] can explain neutrino masses at the one loop level with a DM candidate. The above two models provide the interesting connection between physics of neutrino and DM. Many other types of radiative neutrino mass models with DM have been considered in Refs. [7–48], and those with a non-Abelian discrete symmetry have been proposed in Refs. [49–54]. Recently, models which generate both masses of charged-leptons and neutrinos at the loop level have also been constructed in Refs. [55–57].

Among the various neutrino mass models, the Zee-Babu model mentioned in the above is constructed in a quite simple way, where isospin singlet singly- and doubly-charged scalar fields are added to the SM. However, this model does not have a DM candidate, because all the new particles are electromagnetically charged. In addition, it has been found that the lower bound on the masses of new charged scalar bosons are given between 1 and 2 TeV from the constraints of the most recent experimental data such as neutrino mixing with non-zero θ_{13} ¹ and $\mu \rightarrow e\gamma$ with a perturbativity requirement, which makes difficult to directly discover these new particles at the LHC even with the 14 TeV collision energy [58]. Similar mass bounds have also been shown in

¹ Analysis with the non-zero θ_{13} in the Zee-Babu model has also been performed in Refs. [59, 60].

Ref. [61], in which authors have also taken into account the recent Higgs boson search data at the LHC.

In this paper, we extend the Zee-Babu model so as to include a DM candidate by introducing a discrete Z_2 symmetry to the model². In order to enclose the two-loop diagram, we need to add Z_2 odd fields; i.e., vector-like singly-charged leptons and an isospin doublet scalar field. A DM candidate is then obtained as the lightest neutral component of the doublet scalar field. In this model, the vector-like leptons play a crucial role not only to explain neutrino masses but also the discrepancy between the experimental value of the muon anomalous magnetic moment (muon $g - 2$) and its prediction in the SM [62, 63]. We find that the mass of vector-like leptons to be slightly above 300 GeV is favored to explain the muon $g - 2$, which is not excluded by the current experimental data.

We then discuss the collider phenomenology, especially focusing on the production and decay of doubly-charged scalar bosons at the LHC. The doubly-charged scalar bosons can mainly decay into the same-sign dilepton with the same-flavour and missing transverse momentum due to the structure of neutrino mass matrix. This signal process is completely different with that from doubly-charged scalar bosons in the original Zee-Babu model and the Higgs triplet model (HTM) [64–68] which contains isospin triplet scalar field, and one of its components corresponds to the doubly-charged state.

This paper is organized as follows. In Sec. II, we show our model building including the particle contents, discussion of DM and the constraints from the oblique parameters. In Sec. III, we calculate neutrino mass matrix and the muon $g - 2$. Numerical evaluation of these observables is also given by using the current data for the neutrino masses and mixing. In Sec. IV, the collider phenomenology of the new particles is discussed. Summary and conclusion are given in Sec. V.

II. THE MODEL

² The supersymmetric extension of the Zee-Babu model has been built in Ref. [10], where a DM candidate is obtained as the lightest neutral R-parity odd particle.

	Lepton Fields				Scalar Fields			
	L_L^i	e_R^i	E_L^α	E_R^α	Φ	η	χ^+	κ^{++}
$SU(2)_L$	2	1	1	1	2	2	1	1
$U(1)_Y$	-1/2	-1	-1	-1	+1/2	+1/2	+1	+2
Z_2	+	+	-	-	+	-	-	+

TABLE I: Contents of lepton and scalar fields and their charge assignment under the $SU(2)_L \times U(1)_Y \times Z_2$ symmetry. The indices i ($=1-3$) and α ($=1-3$) denote the flavour for the SM leptons L_L and e_R and the new vector-like leptons E_L and E_R , respectively.

A. Lagrangian

We extend the two-loop induced radiative neutrino mass model proposed by Zee and Babu in Ref. [4] so as to contain a DM candidate by introducing an unbroken discrete Z_2 symmetry. The particle contents and the charge assignment are shown in Table I. We add vector-like charged leptons E_R^α and E_L^α with three flavours; i.e., $\alpha=1-3$. For the scalar sector, we introduce an $SU(2)_L$ doublet η , singly-charged singlet χ^\pm and doubly-charged singlet $\kappa^{\pm\pm}$ fields. Among these new fields, only $\kappa^{\pm\pm}$ are assigned to be Z_2 even. A DM candidate can then be obtained as the lightest neutral Z_2 odd particle; namely, a neutral component of η .

New terms in the Lagrangian for lepton Yukawa interactions and the scalar potential under the $SU(2)_L \times U(1)_Y \times Z_2$ invariance are given by

$$-\mathcal{L}_Y = +(y_\eta)_{i\alpha} \overline{L_L^i} \eta E_R^\alpha + (y_R)_{\alpha\beta} \overline{E_R^{c\alpha}} E_R^\beta \kappa^{++} + (y_L)_{\alpha\beta} \overline{E_L^{c\alpha}} E_L^\beta \kappa^{++} + M_{E^\alpha} \overline{E_L^\alpha} E_R^\alpha + \text{h.c.}, \quad (\text{II.1})$$

$$\begin{aligned} \mathcal{V} = & M_\Phi^2 |\Phi|^2 + M_\eta^2 |\eta|^2 + M_\chi^2 |\chi^+|^2 + M_\kappa^2 |\kappa^{++}|^2 \\ & + (\mu \Phi \eta \chi^- + \mu_\kappa \chi^- \chi^- \kappa^{++} + \text{h.c.}) \\ & + \lambda_1 |\Phi|^4 + \lambda_2 |\eta|^4 + \lambda_3 |\Phi|^2 |\eta|^2 + \lambda_4 (\Phi^\dagger \eta) (\eta^\dagger \Phi) + [\lambda_5 (\Phi^\dagger \eta)^2 + \text{h.c.}] \\ & + \lambda_{\Phi\chi} |\Phi|^2 |\chi^+|^2 + \lambda_{\Phi\kappa} |\Phi|^2 |\kappa^{++}|^2 \\ & + \lambda_{\eta\chi} |\eta|^2 |\chi^+|^2 + \lambda_{\eta\kappa} |\eta|^2 |\kappa^{++}|^2 + \lambda_{\chi\kappa} |\chi^+|^2 |\kappa^{++}|^2 + \lambda_\chi |\chi^+|^4 + \lambda_\kappa |\kappa^{++}|^4, \end{aligned} \quad (\text{II.2})$$

where y_L and y_R are the symmetric 3×3 complex matrices. In the scalar potential, μ , μ_κ and λ_5 can be chosen to be real without any loss of generality by renormalizing the phases to scalar bosons. Notice here that although the $(\overline{e_R^{ci}} e_R^j \kappa^{++} + \text{h.c.})$ terms are allowed in general³, they do not

³ We can forbid these terms by introducing an additional $U(1)$ symmetry. However, such a symmetry also forbids the λ_5 term in the potential in Eq. (II.2) which is necessary to avoid the constraint from the direct detection experiment for DM.

contribute to neutrino mass generations. We thus neglect these terms for simplicity throughout the paper.

After the electroweak symmetry breaking, the scalar fields can be parameterized as

$$\Phi = \begin{bmatrix} G^+ \\ \frac{1}{\sqrt{2}}(v + h + iG^0) \end{bmatrix}, \quad \eta = \begin{bmatrix} \eta^+ \\ \frac{1}{\sqrt{2}}(\eta_R + i\eta_I) \end{bmatrix}. \quad (\text{II.3})$$

where $v \simeq 246$ GeV is the vacuum expectation value (VEV) of the Higgs doublet, and G^\pm and G^0 are respectively the Nambu-Goldstone bosons which are absorbed by the longitudinal components of W^\pm and Z bosons. The other scalar fields are not supposed to have a non-zero VEV, otherwise the electromagnetic interactions or Z_2 symmetry spontaneously breaks down.

The mass of the Higgs boson h is obtained after taking the vacuum condition; i.e., $\partial\mathcal{V}/\partial\Phi|_{\text{VEV}} = 0$ just like the SM Higgs boson as $m_h^2 = 2\lambda_1 v^2$. In our model, only the singly-charged scalar states η^\pm and χ^\pm can mix each other among the new scalar bosons. The mass matrix for the singly-charged scalar states M_\pm^2 in the basis of (η^\pm, χ^\pm) is given by

$$M_\pm^2 = \begin{pmatrix} M_\eta^2 + \frac{v^2}{2}\lambda_3 & \frac{\mu v}{\sqrt{2}} \\ \frac{\mu v}{\sqrt{2}} & M_\chi^2 + \frac{v^2}{2}\lambda_{\Phi\chi} \end{pmatrix}. \quad (\text{II.4})$$

The mass eigenstates H_1^\pm and H_2^\pm are defined by introducing the mixing angle θ as

$$\begin{pmatrix} \eta^\pm \\ \chi^\pm \end{pmatrix} = \begin{pmatrix} \cos\theta & -\sin\theta \\ \sin\theta & \cos\theta \end{pmatrix} \begin{pmatrix} H_1^\pm \\ H_2^\pm \end{pmatrix}, \quad (\text{II.5})$$

where θ and the mass eigenvalues are given by

$$m_{H_1^\pm}^2 = (M_\pm^2)_{11} \cos^2\theta + (M_\pm^2)_{22} \sin^2\theta + (M_\pm^2)_{12} \sin 2\theta, \quad (\text{II.6})$$

$$m_{H_2^\pm}^2 = (M_\pm^2)_{11} \sin^2\theta + (M_\pm^2)_{22} \cos^2\theta - (M_\pm^2)_{12} \sin 2\theta, \quad (\text{II.7})$$

$$\tan 2\theta = \frac{2(M_\pm^2)_{12}}{(M_\pm^2)_{11} - (M_\pm^2)_{22}}. \quad (\text{II.8})$$

All the other masses of scalar bosons are calculated as

$$m_{\kappa^{\pm\pm}}^2 = M_\kappa^2 + \frac{1}{2}\lambda_{\Phi\kappa}v^2, \quad (\text{II.9})$$

$$m_{\eta_R}^2 = M_\eta^2 + \frac{1}{2}(\lambda_3 + \lambda_4 + 2\lambda_5)v^2, \quad (\text{II.10})$$

$$m_{\eta_I}^2 = M_\eta^2 + \frac{1}{2}(\lambda_3 + \lambda_4 - 2\lambda_5)v^2. \quad (\text{II.11})$$

B. Dark Matter

The neutral component of η is the unique DM candidate in the model. Taking $\lambda_5 > 0$, the DM can be identified as η_I which should satisfy the observed thermal relic density [69]. The DM mass is limited as $m_{\eta_I} \lesssim 80$ GeV and $m_{\eta_I} \gtrsim 500$ GeV from the constraint of thermal relic density of DM [70, 71]. When the DM is in the low mass region $m_{\eta_I} \lesssim 80$ GeV (below the W or Z threshold), the main annihilation process is $\eta_I \eta_I \rightarrow h \rightarrow f \bar{f}$ where $b \bar{b}$ is dominant in the final state fermions $f \bar{f}$ due to the size of the Yukawa coupling. In addition to the annihilation process, the co-annihilation with η_R mediated by Z boson, $\eta_R \eta_I \rightarrow Z \rightarrow f \bar{f}$ is effective if the mass difference among them is less than around 10%. The flavor of the final state fermions are universal unlike the annihilation process. Typically the DM mass should be around the SM Higgs resonance; i.e., $m_h/2 \simeq 63$ GeV, to satisfy the thermal DM relic density in the low DM mass region. On the other hand, the annihilation processes $\eta_I \eta_I \rightarrow W^+ W^-$, ZZ and hh can be dominant when the DM mass is above the thresholds. In the region of the DM mass $80 \text{ GeV} \lesssim m_{\eta_I} \lesssim 500 \text{ GeV}$, the predicted relic density is strongly suppressed since the cross section which is fixed by the gauge coupling is too large. We are interested in the low DM mass region because such a low DM mass is favored from inducing the large muon anomalous magnetic moment as will be discussed later. Thus the DM mass is fixed to $m_h/2$ in the following discussion.

There is the constraint from direct detection experiments since the elastic scattering process with nuclei is induced via Higgs boson exchange. The relevant parameters in the model are λ_3 , λ_4 and λ_5 , and they are roughly restricted as $\lambda_3 + \lambda_4 - \lambda_5 \lesssim 0.03$ in the low DM mass region [71] from the recent LUX experiment [72]. Moreover, magnitude of the mass degeneracy between η_R and η_I is constrained because the inelastic scattering process $\eta_I N \rightarrow \eta_R N$ can occur via Z boson exchange if the mass splitting is small enough. The mass splitting as small as 100 keV is typically ruled out from the Z exchange process [73].

C. S , T and U Parameters

We consider the constraints from the electroweak S , T and U parameters proposed by Peskin and Takeuchi [74]. The new contributions to the S , T and U parameters are given by

$$S_{\text{new}} = \frac{1}{4\pi m_Z^2} \left[c_\theta^2 (c_\theta^2 - 2) F(m_Z^2; m_{H_1^\pm}, m_{H_1^\pm}) + s_\theta^2 (s_\theta^2 - 2) F(m_Z^2; m_{H_2^\pm}, m_{H_2^\pm}) \right. \\ \left. + 2s_\theta^2 c_\theta^2 [F(m_Z^2; m_{H_1^\pm}, m_{H_2^\pm}) - F(0; m_{H_1^\pm}, m_{H_2^\pm})] + [F(m_Z^2; m_{\eta_R}, m_{\eta_I}) - F(0; m_{\eta_R}, m_{\eta_I})] \right], \quad (\text{II.12})$$

$$T_{\text{new}} = \frac{1}{16\pi^2 \alpha_{\text{em}} v^2} \left[c_\theta^2 F(0; m_{H_1^\pm}, m_{\eta_R}) + c_\theta^2 F(0; m_{H_1^\pm}, m_{\eta_I}) + s_\theta^2 F(0; m_{H_2^\pm}, m_{\eta_R}) \right. \\ \left. + s_\theta^2 F(0; m_{H_2^\pm}, m_{\eta_I}) - F(0; m_{\eta_I}, m_{\eta_R}) - 2s_\theta^2 c_\theta^2 F(0; m_{H_1^\pm}, m_{H_2^\pm}) \right], \quad (\text{II.13})$$

$$U_{\text{new}} = -\frac{1}{4\pi m_Z^2} \left\{ c_\theta^4 F(m_Z^2; m_{H_1^\pm}, m_{H_1^\pm}) + s_\theta^4 F(m_Z^2; m_{H_2^\pm}, m_{H_2^\pm}) \right. \\ \left. + 2s_\theta^2 c_\theta^2 [F(m_Z^2; m_{H_1^\pm}, m_{H_2^\pm}) - F(0; m_{H_1^\pm}, m_{H_2^\pm})] + [F(m_Z^2; m_{\eta_R}, m_{\eta_I}) - F(0; m_{\eta_R}, m_{\eta_I})] \right. \\ \left. - \frac{m_Z^2}{m_W^2} \left[c_\theta^2 \left(F(m_W^2; m_{H_1^\pm}, m_{\eta_R}) - F(0; m_{H_1^\pm}, m_{\eta_R}) + F(m_W^2; m_{H_1^\pm}, m_{\eta_I}) - F(0; m_{H_1^\pm}, m_{\eta_I}) \right) \right. \right. \\ \left. \left. + s_\theta^2 \left(F(m_W^2; m_{H_2^\pm}, m_{\eta_R}) - F(0; m_{H_2^\pm}, m_{\eta_R}) + F(m_W^2; m_{H_2^\pm}, m_{\eta_I}) - F(0; m_{H_2^\pm}, m_{\eta_I}) \right) \right] \right\}, \quad (\text{II.14})$$

where $c_\theta \equiv \cos \theta$ and $s_\theta \equiv \sin \theta$, and $\alpha_{\text{em}} \simeq 1/137$ is the electromagnetic fine structure constant.

The function $F(p^2; m_1, m_2)$ is given by

$$F(p^2; m_1, m_2) = \int_0^1 dx \left[(2x - 1)(m_1^2 - m_2^2) + (2x - 1)^2 p^2 \right] \ln \left[x m_1^2 + (1 - x) m_2^2 - x(1 - x) p^2 \right], \quad (\text{II.15})$$

This function is reduced to the simple form in the case of $p^2 = 0$ as

$$F(0; m_1, m_2) = \frac{m_1^2 + m_2^2}{2} - \frac{m_1^2 m_2^2}{m_1^2 - m_2^2} \ln \left(\frac{m_1^2}{m_2^2} \right), \quad (\text{II.16})$$

which gives zero in the case of $m_1 = m_2$. The experimental deviations from the SM predictions in the S and T parameters under $m_h = 126$ GeV and $U = 0$ are given by [75]⁴

$$S_{\text{new}} = 0.05 \pm 0.09, \quad T_{\text{new}} = 0.08 \pm 0.07, \quad (\text{II.17})$$

where the correlation factor between S_{new} and T_{new} is +0.91.

⁴ Typically, the magnitude of U_{new} is smaller than 0.01 when the prediction of S_{new} and T_{new} parameters are inside the 95% CL allowed region by the data.

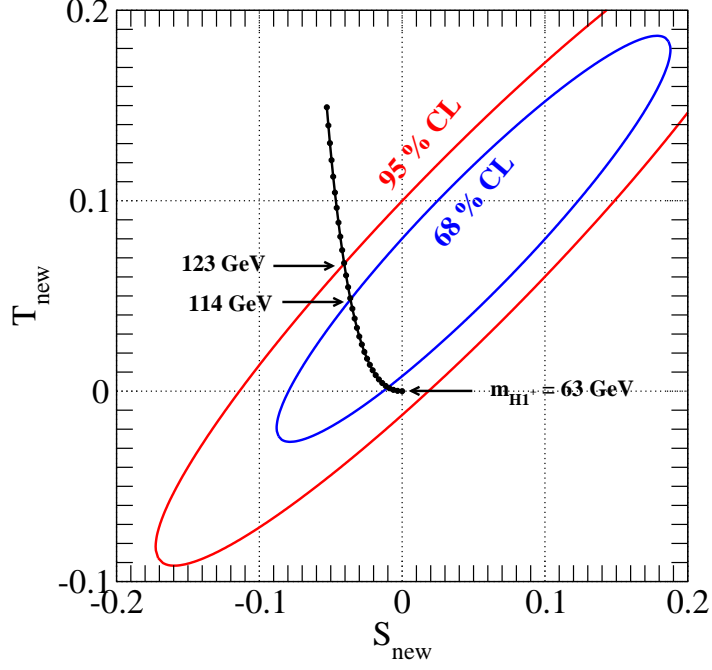


FIG. 1: Contour plot for the S_{new} and T_{new} parameters. We take $\theta = 0$ and $m_{\eta_R} = m_{\eta_I} = 63$ GeV. The blue and red ellipses denote the 68% and 95% CL limits, respectively, for the S and T parameters. The black dots show the prediction of the S_{new} and T_{new} parameters, where $m_{H_1^\pm}$ is valid from 63 GeV to 153 GeV with the 3 GeV interval.

In Fig. 1, we show the prediction of the S_{new} and T_{new} parameters. The 68% and 95% CL limits for the S_{new} and T_{new} parameters are respectively denoted by the blue and red ellipses. We take $\theta = 0$ and $m_{\eta_R} = m_{\eta_I} = 63$ GeV in this plot. In that case, S_{new} and T_{new} are determined by fixing $m_{H_1^\pm}$ which corresponds to the mass of η^\pm . The prediction on the $S_{\text{new}}-T_{\text{new}}$ plane changes from the origin to the left-upper edge along the black curve when $m_{H_1^\pm}$ is valid from 63 GeV to 153 GeV. From this figure, we obtain the upper limit on $m_{H_1^\pm}$ to be 114 GeV and 123 GeV with the 68% CL and 95% CL, respectively. The upper limit on $m_{H_1^\pm}$ will be relaxed with several dozens GeV if $U_{\text{new}} \neq 0$ is taken into account [75].

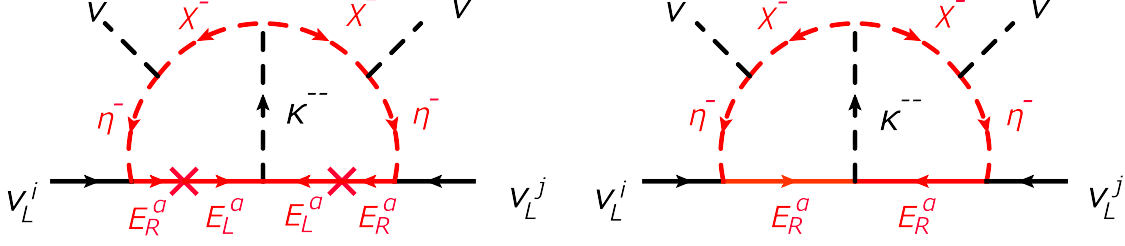


FIG. 2: Feynman diagrams for the neutrino mass generation at the two-loop level. Particles indicated by the red color have the Z_2 odd parity.

III. NEUTRINO MASS AND MUON ANOMALOUS MAGNETIC MOMENT

A. Neutrino mass matrix

The Majorana neutrino mass matrix m_ν is derived at two-loop level from the diagrams depicted in Fig. 2. The contribution of the left diagram is given by

$$\begin{aligned}
 (m_\nu^L)_{ij} = & \frac{\mu_\kappa \sin^2 2\theta}{4(16\pi^2)^2} \sum_{\alpha=1}^3 \sum_{\beta=1}^3 \left[\frac{(y_\eta)_{i\alpha} M_{E^\alpha} (y_L)_{\alpha\beta}^* (M_{E^\beta}) (y_\eta)_{\beta j}}{M_{E^\alpha}^2} \right] \\
 & \times \left[F_L \left(\frac{m_{H_1^\pm}^2}{M_{E^\alpha}^2}, \frac{m_{\kappa^{\pm\pm}}^2}{M_{E^\alpha}^2}, \frac{m_{H_1^\pm}^2}{M_{E^\alpha}^2}, \frac{M_{E^\beta}^2}{M_{E^\alpha}^2} \right) - F_L \left(\frac{m_{H_2^\pm}^2}{M_{E^\alpha}^2}, \frac{m_{\kappa^{\pm\pm}}^2}{M_{E^\alpha}^2}, \frac{m_{H_1^\pm}^2}{M_{E^\alpha}^2}, \frac{M_{E^\beta}^2}{M_{E^\alpha}^2} \right) \right. \\
 & \left. - F_L \left(\frac{m_{H_1^\pm}^2}{M_{E^\alpha}^2}, \frac{m_{\kappa^{\pm\pm}}^2}{M_{E^\alpha}^2}, \frac{m_{H_2^\pm}^2}{M_{E^\alpha}^2}, \frac{M_{E^\beta}^2}{M_{E^\alpha}^2} \right) + F_L \left(\frac{m_{H_2^\pm}^2}{M_{E^\alpha}^2}, \frac{m_{\kappa^{\pm\pm}}^2}{M_{E^\alpha}^2}, \frac{m_{H_2^\pm}^2}{M_{E^\alpha}^2}, \frac{M_{E^\beta}^2}{M_{E^\alpha}^2} \right) \right], \quad (\text{III.1})
 \end{aligned}$$

and that of the right diagram is given by

$$\begin{aligned}
 (m_\nu^R)_{ij} = & \frac{\mu_\kappa \sin^2 2\theta}{4(16\pi^2)^2} \sum_{\alpha=1}^3 \sum_{\beta=1}^3 [(y_\eta)_{i\alpha} (y_R)_{\alpha\beta}^* (y_\eta)_{\beta j}] \\
 & \times \left[-F_R \left(\frac{m_{H_1^\pm}^2}{M_{E^\alpha}^2}, \frac{m_{\kappa^{\pm\pm}}^2}{M_{E^\alpha}^2}, \frac{m_{H_1^\pm}^2}{M_{E^\alpha}^2}, \frac{M_{E^\beta}^2}{M_{E^\alpha}^2} \right) + F_R \left(\frac{m_{H_1^\pm}^2}{M_{E^\alpha}^2}, \frac{m_{\kappa^{\pm\pm}}^2}{M_{E^\alpha}^2}, \frac{m_{H_2^\pm}^2}{M_{E^\alpha}^2}, \frac{M_{E^\beta}^2}{M_{E^\alpha}^2} \right) \right. \\
 & \left. + F_R \left(\frac{m_{H_2^\pm}^2}{M_{E^\alpha}^2}, \frac{m_{\kappa^{\pm\pm}}^2}{M_{E^\alpha}^2}, \frac{m_{H_1^\pm}^2}{M_{E^\alpha}^2}, \frac{M_{E^\beta}^2}{M_{E^\alpha}^2} \right) - F_R \left(\frac{m_{H_2^\pm}^2}{M_{E^\alpha}^2}, \frac{m_{\kappa^{\pm\pm}}^2}{M_{E^\alpha}^2}, \frac{m_{H_2^\pm}^2}{M_{E^\alpha}^2}, \frac{M_{E^\beta}^2}{M_{E^\alpha}^2} \right) \right]. \quad (\text{III.2})
 \end{aligned}$$

The loop functions F_L and F_R are computed as

$$F_L(X_1, X_2, X_3, X_4) = \int_0^1 dx dy dz \frac{\delta(x+y+z-1)}{z(z-1)} \int_0^1 dx' dy' dz' \frac{\delta(x'+y'+z'-1)}{x'+y'X_1 - z'\Delta(X_2, X_3, X_4)}, \quad (\text{III.3})$$

$$F_R(X_1, X_2, X_3, X_4) = 2 \int_0^1 dx dy dz \frac{\delta(x+y+z-1)}{z-1} \int_0^1 dx' dy' dz' \delta(x'+y'+z'-1) \times \ln [x' + y'X_1 - z'\Delta(X_2, X_3, X_4)], \quad (\text{III.4})$$

where

$$\Delta(X_2, X_3, X_4) = \frac{xX_4 + yX_3 + zX_2}{z(z-1)}. \quad (\text{III.5})$$

The total neutrino mass matrix is given by $(m_\nu)_{ij} = (m_\nu^L)_{ij} + (m_\nu^R)_{ij}$. Notice here that the contribution from the left figure in Fig. 2 is reduced to the neutrino mass matrix given in the original Zee-Babu model in the limit of $M_{E^\alpha} \rightarrow 0$ [76].

When we assume that y_η is proportional to the unit matrix; i.e., $(y_\eta)_{i\alpha} = y_\eta \times \mathbf{1}_{3 \times 3}$, and all the masses for E^α are degenerate; $M_{E^\alpha} (\alpha = 1, 2, 3) = M_E$, the neutrino mass matrix is simply rewritten as

$$(m_\nu)_{ij} = C_L(y_L)_{ij} - C_R(y_R)_{ij}, \quad (\text{III.6})$$

where

$$C_{L,R} = \frac{\mu_\kappa}{4(16\pi^2)^2} y_\eta^2 \sin^2 2\theta \left[F_{L,R} \left(x_{H_1^\pm}, x_{\kappa^\pm\pm}, x_{H_1^\pm}, 1 \right) - F_{L,R} \left(x_{H_2^\pm}, x_{\kappa^\pm\pm}, x_{H_1^\pm}, 1 \right) - F_{L,R} \left(x_{H_1^\pm}, x_{\kappa^\pm\pm}, x_{H_2^\pm}, 1 \right) + F_{L,R} \left(x_{H_2^\pm}, x_{\kappa^\pm\pm}, x_{H_2^\pm}, 1 \right) \right], \text{ with } x_\varphi = m_\varphi^2/M_E^2. \quad (\text{III.7})$$

The neutrino mass matrix is diagonalized by introducing the Pontecorvo-Maki-Nakagawa-Sakata matrix U_{PMNS} as [77]

$$U_{\text{PMNS}}^T m_\nu U_{\text{PMNS}} = \text{diag}(m_1, m_2, m_3). \quad (\text{III.8})$$

By using the following best fit values of the neutrino mixing angles and squared mass differences assuming the normal (inverted) mass hierarchy [78];

$$\sin^2 \theta_{12} = 0.323 (0.323), \quad \sin^2 \theta_{23} = 0.567 (0.573), \quad \sin^2 \theta_{13} = 0.0234 (0.0240), \quad (\text{III.9})$$

$$\Delta m_{21}^2 = 7.60 (7.60) \times 10^{-5} \text{ eV}^2, \quad |\Delta m_{31}|^2 = 2.48 (2.38) \times 10^{-3} \text{ eV}^2, \quad (\text{III.10})$$

we obtain the U_{PMNS} matrix elements as

$$U_{\text{PMNS}} = \begin{pmatrix} 0.813 (0.813) & 0.562 (0.561) & 0.153 (0.155) \\ -0.469 (-0.468) & 0.476 (0.471) & 0.744 (0.748) \\ 0.345 (0.347) & -0.677 (-0.680) & 0.650 (0.646) \end{pmatrix}, \quad (\text{III.11})$$

where we neglect the CP-violating phase, which is experimentally allowed within the $2\text{-}\sigma$ level [78]. In addition, using the central value of the sum of neutrino masses 0.36 eV [79], the eigenvalues for the neutrino masses are determined in the normal (inverted) hierarchy as

$$m_1 = 0.116 (0.124) \text{ eV}, \quad m_2 = 0.117 (0.123) \text{ eV}, \quad m_3 = 0.127 (0.113) \text{ eV}. \quad (\text{III.12})$$

From Eqs. (III.8), (III.11) and (III.12), and taking $y_L = y_R (= \bar{y})$, we obtain the matrix elements of \bar{y} in the normal (inverted) hierarchy;

$$\begin{aligned} \bar{y}_{ij} &= \frac{m_{\text{max}}}{C_L - C_R} U_{\text{PMNS}} \text{diag}(m_1/m_{\text{max}}, m_2/m_{\text{max}}, m_3/m_{\text{max}}) U_{\text{PMNS}}^T \\ &= \frac{m_{\text{max}}}{C_L - C_R} \begin{pmatrix} 0.922 (0.997) & 0.00985 (-0.0104) & 0.00703 (-0.00744) \\ 0.00985 (-0.0104) & 0.965 (0.952) & 0.0381 (-0.0397) \\ 0.00703 (-0.00744) & 0.0381 (-0.0397) & 0.955 (0.964) \end{pmatrix}, \end{aligned} \quad (\text{III.13})$$

where m_{max} is the largest eigenvalue of neutrino masses; i.e., $m_{\text{max}} = m_3$ (m_1). The order of magnitude of the parameter $|C_L - C_R|$ is estimated as

$$|C_L - C_R| = 0.1 \text{ eV} \times \left(\frac{y_\eta}{1.0} \right)^2 \left(\frac{|\mu_\kappa|}{1 \text{ TeV}} \right) \left(\frac{\sin 2\theta}{10^{-4}} \right)^2, \quad (\text{III.14})$$

where typical magnitudes of the loop functions $F_{L,R}$ are fixed to be $\mathcal{O}(1)$.

B. Muon anomalous magnetic moment

The muon anomalous magnetic moment (muon $g-2$) has been measured at Brookhaven National Laboratory. The current average of the experimental results is given by [80]

$$a_\mu^{\text{exp}} = 11659208.0(6.3) \times 10^{-10}.$$

It has been well known that there is a discrepancy between the experimental data and the prediction in the SM. The difference $\Delta a_\mu \equiv a_\mu^{\text{exp}} - a_\mu^{\text{SM}}$ was calculated in Ref. [62] as

$$\Delta a_\mu = (29.0 \pm 9.0) \times 10^{-10}, \quad (\text{III.15})$$

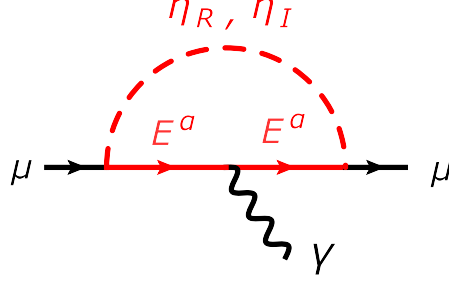


FIG. 3: Feynman diagram for the new contribution to the muon $g - 2$.

and it was also derived in Ref. [63] as

$$\Delta a_\mu = (33.5 \pm 8.2) \times 10^{-10}. \quad (\text{III.16})$$

The above results given in Eqs. (III.15) and (III.16) correspond to 3.2σ and 4.1σ deviations, respectively.

In our model, there are new contributions to Δa_μ as shown in Fig. 3. These contributions are calculated as

$$\Delta a_\mu = \frac{1}{32\pi^2} \sum_{\alpha=1}^3 |y_\eta^{2\alpha}|^2 \left(\frac{m_\mu}{M_{E^\alpha}} \right)^2 \left[G \left(\frac{m_{\eta_R}^2}{M_{E^\alpha}^2} \right) + G \left(\frac{m_{\eta_I}^2}{M_{E^\alpha}^2} \right) \right], \quad (\text{III.17})$$

where

$$G(x) = \frac{1 - 6x + 3x^2 + 2x^3 - 6x^2 \ln x}{6(1-x)^4}. \quad (\text{III.18})$$

Under the same assumption taken in the previous subsection, we obtain

$$\Delta a_\mu = \frac{y_\eta^2}{16\pi^2} \left(\frac{m_\mu}{M_E} \right)^2 G \left(\frac{m_{\eta^0}^2}{M_E^2} \right), \quad (\text{III.19})$$

where we neglect the mass difference between η_R and η_I ; i.e., $m_{\eta_R} = m_{\eta_I} \equiv m_{\eta^0}$.

In Fig. 4, the prediction of Δa_μ is shown on the M_E - y_η plane in the case of $m_{\eta^0} = 63$ GeV. From Eqs. (III.15) and (III.16), we can obtain the lower and upper limits on Δa_μ as $1.1 \times 10^{-9} < \Delta a_\mu < 5.0 \times 10^{-9}$ by allowing up to the $2\text{-}\sigma$ error. In the blue shaded regions, the prediction is inside the above limit. Furthermore, if we require perturbativity of the coupling constant y_η ; i.e., $y_\eta^2/(4\pi) \leq 1$, the upper limit for y_η can be set, which is denoted by the horizontal dashed line. When we take the maximal allowed value of y_η from perturbativity, the region of $150 \text{ GeV} \lesssim M_E \lesssim 350 \text{ GeV}$ is favored by Δa_μ . In the next section, we discuss the constraint on M_E from the current LHC data.

In the end of this section, we comment on new contributions to the lepton flavor violating (LFV) processes such as $\mu \rightarrow e\gamma$ in our model. In general, we can consider diagrams which contribute

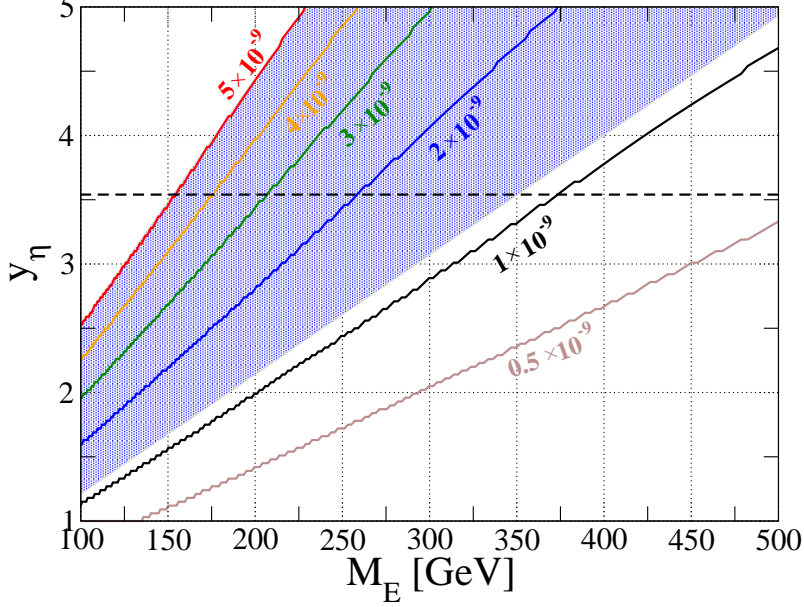


FIG. 4: Contour plots for Δa_μ using Eq. (III.19) on the M_E - y_η plane in the case of $m_{\eta^0} = 63$ GeV. In the shaded regions, $1.1 \times 10^{-9} < \Delta a_\mu < 5.0 \times 10^{-9}$ is satisfied, where the lower and upper limits on Δa_μ are respectively derived from Eqs. (III.15) and (III.16) with taking into account the $2\text{-}\sigma$ error. The horizontal dashed line denotes the upper limit for y_η from the requirement of perturbativity; i.e., $y_\eta^2/(4\pi) \leq 1$.

to the LFV processes by replacing the external muons shown in Fig. 3 with charged-leptons with different flavors with each other. Such a contribution is proportional to the off-diagonal element of the y_η coupling, so that we can avoid constraints from the LFV data as long as we take the diagonal structure of y_η .

IV. COLLIDER PHENOMENOLOGY

In this section, we discuss the collider phenomenology of our model. First of all, we specify the mass spectrum according to the previous sections. From the physics of DM, we set the mass of the lightest neutral Z_2 odd scalar boson η_I to be 63 GeV. The mass of η_R must be larger than that of η_I at least order of 100 keV from the direct detection experiments for DM. In addition in order to reproduce the collect order of neutrino masses, the mixing angle θ has to be as small as $\mathcal{O}(10^{-4})$ as seen Eq. (III.14). Such a small mass difference between η_I and η_R and small angle θ can be neglected in the collider phenomenology. We thus take $m_{\eta_R} = m_{\eta_I}$ and $\theta = 0$ for simplicity. In that case, from the S and T parameters, the upper limit for the mass of $\eta^\pm (= m_{H^\pm_1})$ is given to be 123 GeV with the 95 % CL (see Fig. 1).

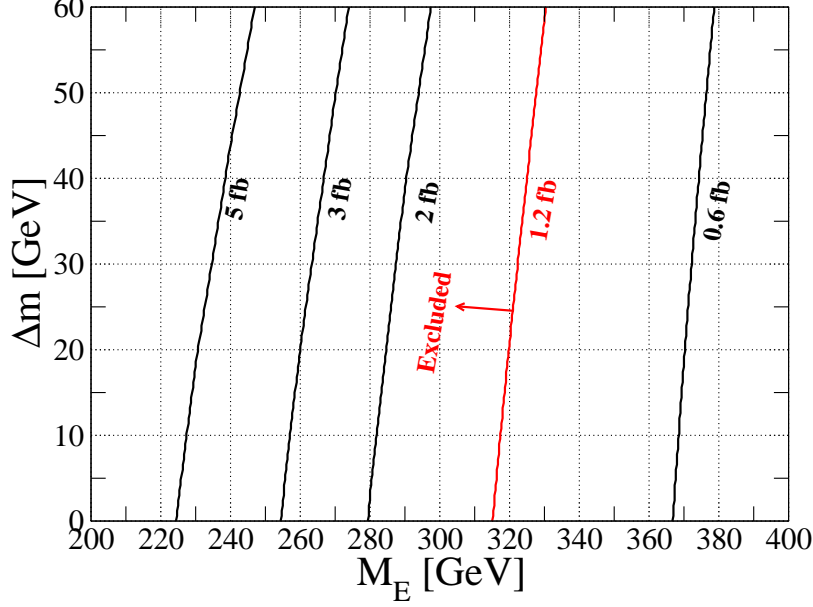


FIG. 5: Contour plots for the cross section of the $pp \rightarrow E_\alpha^+ E_\alpha^- \rightarrow \ell_\alpha^+ \ell_\alpha^- \eta^0 \eta^0$ process for each lepton flavour α on the $M_E - \Delta m$ ($\equiv m_{\eta^\pm} - m_{\eta^0}$) with the collision energy to be 8 TeV. We fix m_{η^0} to be 63 GeV. The red contour denotes the cross section of 1.2 fb which corresponds to the upper limit from the slepton search performed in Ref. [81].

The mass of vector-like charged leptons E^α can be constrained from slepton searches at the LHC in the following way. In Ref. [81], the bound on the slepton masses has been given from the search for $pp \rightarrow \tilde{\ell}^+ \tilde{\ell}^- \rightarrow \ell^+ \ell^- \tilde{\chi}^0 \tilde{\chi}^0$ process, where $\tilde{\ell}^\pm$ and $\tilde{\chi}^0$ are the charged slepton and the neutralino, respectively, and ℓ is e or μ . For the case where produced sleptons are purely left-handed, the lower limit on the mass of $\tilde{\ell}$ has been given to be about 300 GeV from the data with the integrated luminosity to be 20.3 fb^{-1} and the collision energy to be 8 TeV. In our model, there are two decay modes of E^α ; i.e., $E^\alpha \rightarrow \nu^\alpha \eta^\pm$ and $E^\alpha \rightarrow \ell^{\alpha\pm} \eta^0$ (η^0 is η_R or η_I) via the Yukawa coupling y_η which is assumed to be proportional to the unit matrix $(y_\eta)_{i\alpha} = y_\eta \times \mathbf{1}_{3 \times 3}$. Therefore, the similar final state as in the slepton pair production is obtained by $pp \rightarrow E^{\alpha+} E^{\alpha-} \rightarrow \ell^+ \ell^- \eta^0 \eta^0$. The cross section of this process can be estimated as

$$\sigma(pp \rightarrow \ell^+ \ell^- \eta^0 \eta^0) = \sigma(pp \rightarrow E^{\alpha+} E^{\alpha-}) \times \mathcal{B}(E^{\alpha\pm} \rightarrow \ell^{\alpha\pm} \eta^0)^2, \quad (\text{IV.1})$$

where $\sigma(pp \rightarrow E^{\alpha+} E^{\alpha-})$ is the pair production cross section of E^α , and $\mathcal{B}(E^{\alpha\pm} \rightarrow \ell^{\alpha\pm} \eta^0)$ is the branching fraction for the $E^{\alpha\pm} \rightarrow \ell^{\alpha\pm} \eta^0$ mode. When the mass of left-handed slepton is taken to be 300 GeV, the pair production cross section is calculated to be about 1.2 fb for each flavour of $\tilde{\ell}$, where we use CalcHEP [82] and CTEQ6L for the parton distribution function. We thus can set

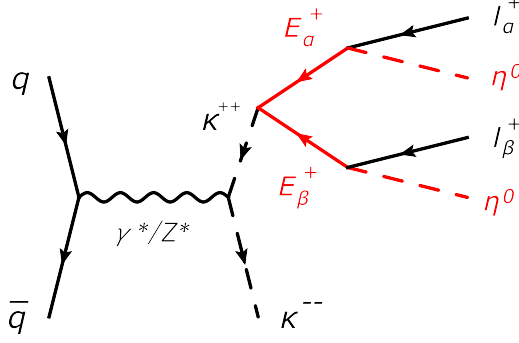


FIG. 6: Feynman diagram for the signal process in the model. The decay of κ^{--} can be the same as that of κ^{++} by replacing ℓ_α^+ with ℓ_α^- .

the lower limit on the mass of E^α by requiring that the cross section $\sigma(pp \rightarrow \ell^+ \ell^- \eta^0 \eta^0)$ does not exceed 1.2 fb.

In Fig. 5, we show the contour plots of the cross section of the process $pp \rightarrow E_\alpha^+ E_\alpha^- \rightarrow \ell_\alpha^+ \ell_\alpha^- \eta^0 \eta^0$ for each lepton flavour α on the $M_E - \Delta m$ ($\equiv m_{\eta^\pm} - m_{\eta^0}$) plane. Again, the cross section is calculated by using **CalcHEP** and **CTEQ6L**. The upper limit on the cross section from the slepton search is shown as the red curve, so that the left region from the red curve is excluded. We can see that the cross section slightly increases as Δm is getting a large value, because the branching fraction of $E_\alpha^\pm \rightarrow \ell_\alpha^\pm \eta^0$ gets a small enhancement. By looking at the red curve, we find that the lower bound on M_E is given as about 315 GeV to 330 GeV depending on the value of Δm . Therefore, there are allowed regions by the LHC bound, where the discrepancy in the muon $g - 2$ can be explained.

In the following discussion, we take $M_E = 315$ GeV and $\Delta m \simeq 0$ ⁵. In addition, we assume that the mass of $\kappa^{\pm\pm}$ is larger than $2M_E$ and χ^\pm are heavier than $\kappa^{\pm\pm}$. In that case, we expect that the event with the same-sign dilepton plus missing transverse momentum appears from the pair production of $\kappa^{\pm\pm}$ as shown in Fig. 6. The cross section of this process is calculated by

$$\begin{aligned} \sigma(pp \rightarrow \ell_\alpha^+ \ell_\beta^+ \cancel{E}_T \kappa^{--}) &= \sigma(pp \rightarrow \kappa^{++} \kappa^{--}) \times \mathcal{B}(\kappa^{++} \rightarrow E_\alpha^+ E_\beta^+) \times \mathcal{B}(E^\pm \rightarrow \ell^\pm \eta^0)^2 \\ &\simeq \frac{1}{4} \sigma(pp \rightarrow \kappa^{++} \kappa^{--}) \times \mathcal{B}(\kappa^{++} \rightarrow E_\alpha^+ E_\beta^+). \end{aligned} \quad (\text{IV.2})$$

where $\sigma(pp \rightarrow \kappa^{++} \kappa^{--})$ is the pair production cross section of $\kappa^{\pm\pm}$, and $\mathcal{B}(\kappa^{++} \rightarrow E_\alpha^+ E_\beta^+)$ is the branching fraction of the $\kappa^{++} \rightarrow E_\alpha^+ E_\beta^+$ mode. Under the assumption of $y_L = y_R$ ($= \bar{y}$) which was

⁵ If we exactly take $\Delta m = 0$, then η^\pm cannot decay into the other particles. If there is the non-zero mass difference, η^\pm can decay into $W^{\pm*} \eta^0$.

Mode (α, β)	(e, e)	(μ, μ)	(τ, τ)	(e, μ)	(e, τ)	(μ, τ)
$\mathcal{B}(\kappa^{++} \rightarrow E_\alpha^+ E_\beta^+) [\%]$	31.5 (35.1)	34.5 (32.0)	33.8 (32.8)	7.20×10^{-3} (7.61×10^{-3})	3.67×10^{-3} (3.91×10^{-3})	0.108 (0.111)
$\sigma(pp \rightarrow \kappa^{++} \kappa^{--}) [\text{fb}]$	0.202 ($m_{\kappa^{\pm\pm}} = 650 \text{ GeV}$)					
$\sigma(pp \rightarrow \ell_\alpha^+ \ell_\beta^+ \cancel{E}_T \kappa^{--})/10^2 [\text{fb}]$	1.59 (1.77)	1.74 (1.62)	1.71 (1.66)	$\simeq 0$ (0)	$\simeq 0$ (0)	$\simeq 0$ (0)
$\sigma(pp \rightarrow \kappa^{++} \kappa^{--}) [\text{fb}]$	0.0690 ($m_{\kappa^{\pm\pm}} = 800 \text{ GeV}$)					
$\sigma(pp \rightarrow \ell_\alpha^+ \ell_\beta^+ \cancel{E}_T \kappa^{--})/10^2 [\text{fb}]$	0.543 (0.615)	0.595 (0.552)	0.583 (0.566)	$\simeq 0$ (0)	$\simeq 0$ (0)	$\simeq 0$ (0)
$\sigma(pp \rightarrow \kappa^{++} \kappa^{--}) [\text{fb}]$	0.0193 ($m_{\kappa^{\pm\pm}} = 1000 \text{ GeV}$)					
$\sigma(pp \rightarrow \ell_\alpha^+ \ell_\beta^+ \cancel{E}_T \kappa^{--})/10^2 [\text{fb}]$	0.152 (0.169)	0.166 (0.154)	0.163 (0.158)	$\simeq 0$ (0)	$\simeq 0$ (0)	$\simeq 0$ (0)

TABLE II: Branching fraction of κ^{++} , the cross section for the pair production of $\kappa^{\pm\pm}$, and that for the process expressed in Eq. (IV.2) are shown with the collision energy to be 14 TeV. The numbers without (with) bracket are the results by using the neutrino mixing data assuming the normal (inverted) hierarchy given in Eq. (III.13).

taken in the previous section, the decay rate of $\kappa^{++} \rightarrow E_\alpha^+ E_\beta^+$ mode is calculated by

$$\Gamma(\kappa^{++} \rightarrow E_\alpha^+ E_\beta^+) = S_{\alpha\beta} \frac{|\bar{y}_{\alpha\beta}|^2}{4\pi} m_{\kappa^{\pm\pm}} \left(1 - \frac{4M_E^2}{m_{\kappa^{\pm\pm}}^2}\right)^{3/2}, \quad (\text{IV.3})$$

where $S_{\alpha\beta} = 2$ (1) for $\alpha \neq \beta$ ($\alpha = \beta$). From the above formula, the branching fraction is simply determined by $\bar{y}_{\alpha\beta}$ as

$$\mathcal{B}(\kappa^{++} \rightarrow E_\alpha^+ E_\beta^+) = \frac{S_{\alpha\beta} |\bar{y}_{\alpha\beta}|^2}{|\bar{y}_{ee}|^2 + |\bar{y}_{\mu\mu}|^2 + |\bar{y}_{\tau\tau}|^2 + 2(|\bar{y}_{e\mu}|^2 + |\bar{y}_{e\tau}|^2 + |\bar{y}_{\mu\tau}|^2)}. \quad (\text{IV.4})$$

Each matrix element of $\bar{y}_{\alpha\beta}$ is given by using the neutrino mixing data as expressed in Eq. (III.13). In Table II, the branching fraction of κ^{++} is listed. Because the Yukawa coupling \bar{y} determined from Eq. (III.13) is almost the unite matrix, the decay of κ^{++} into the same flavour of E_α is dominant. This results in the final state of the signal process shown in Fig. 6 with the same-sign dilepton with the same-flavour and missing transverse energy, and each of three lepton flavours in the final state appears almost the same probability with each other. With the 14 TeV energy at the LHC, the cross section for the pair production ($pp \rightarrow \kappa^{++} \kappa^{--}$) and that for the process expressed in Eq. (IV.2) for each lepton flavour of the final state are also shown in Table II. We can see that about 10 events can be obtained for the same-sign electron or muon and missing transverse energy final states assuming 300 fb^{-1} for the integrated luminosity.

Finally, we comment on signals from doubly-charged scalar bosons from the other models. In the original Zee-Babu model, there are isospin singlet doubly-charged scalar bosons just like $\kappa^{\pm\pm}$ in our model. They can directly decay into the same-sign dilepton without missing energies. Thus, we expect that the sharp peak appears at the mass of doubly-charged scalar bosons in the invariant mass distribution for the same-sign dilepton system [83, 84]. Similar signal with the same-sign dilepton can also appear in the HTM [64–68], in which there are doubly-charged scalar components in the isospin triplet Higgs field. On the other hand, the doubly-charged scalar bosons $\kappa^{\pm\pm}$ in our model do not directly decay into the same-sign dilepton as seen in Fig. 6, whose decay products include missing energies due to DM. The peak in the invariant mass distribution cannot then be seen in that case, and the signal from the decay of $\kappa^{\pm\pm}$ is different from that from doubly-charged scalar bosons in the Zee-Babu model and in the HTM. In the HTM, the doubly-charged scalar bosons can also decay into the same-sign W bosons when the VEV of triplet Higgs field is taken to be larger than about 0.1-1 MeV [85–89]. Such a decay mode provides a final state with the same-sign dilepton plus missing energies due to the leptonic decay of the W bosons. However, the combination of flavour for the same-sign dilepton equally appears due to the universality of leptonic decay of the weak boson. In our model, the same-sign dilepton with the different flavour in the final state is strongly suppressed due to the structure of neutrino mass matrix. Therefore, by measuring the lepton flavour of the same-sign dilepton event, our model can be distinguished from the HTM. One should note that if the interaction we have neglected $\kappa^{++}\bar{e}_i^c e_j$ in the paper exists, eventually the same invariant mass distribution with the other models may be obtained. Thus the assumption that there is no Yukawa coupling $\kappa^{++}\bar{e}_i^c e_j$ is important to see the difference as discussed above.

V. CONCLUSIONS

We have constructed the two-loop induced Zee-Babu type neutrino mass model, in which a DM candidate is included. In our model, the DM is the lighter one of the neutral components of the inert doublet scalar. The DM mass should be around 63 GeV from the view points of the thermal relic density and explanation for the discrepancy in the muon $g - 2$. The discrepancy between the experimental value of the muon $g - 2$ and its prediction in the SM can be explained due to the vector-like charged leptons with the mass of less than about 350 GeV. By taking into account the current smuon search at the LHC, the lower bound on the mass of vector-like leptons has been taken to be about 315 GeV. Therefore, the parameter regions favored by the muon $g - 2$ are

still allowed by the current LHC data. We have discussed the collider phenomenology, especially focusing on the doubly-charged scalar bosons $\kappa^{\pm\pm}$. We have found that the main decay mode of $\kappa^{\pm\pm}$ can be the same-sign dilepton with the same-flavour plus missing transverse momentum due to the structure of neutrino mass matrix. It suggests that measuring an excess of the same-sign dilepton events with the same-flavour, we can distinguish our model from the other models which include doubly-charged scalar bosons such as the original Zee-Babu model and the HTM.

Acknowledgments

Author thanks to Prof. Seungwon Baek for fruitful discussions. T. T. acknowledges support from the European ITN project (FP7-PEOPLE- 2011-ITN, PITN-GA-2011-289442-INVISIBLES). K. Y. was supported in part by the National Science Council of R.O.C. under Grant No. NSC-101-2811-M-008-014.

-
- [1] G. Aad *et al.* [ATLAS Collaboration], Phys. Lett. B **716**, 1 (2012) [arXiv:1207.7214 [hep-ex]].
 - [2] S. Chatrchyan *et al.* [CMS Collaboration], Phys. Lett. B **716**, 30 (2012) [arXiv:1207.7235 [hep-ex]].
 - [3] A. Zee, Phys. Lett. B **93**, 389 (1980) [Erratum-ibid. B **95**, 461 (1980)].
 - [4] A. Zee, Nucl. Phys. B **264**, 99 (1986); K. S. Babu, Phys. Lett. B **203**, 132 (1988).
 - [5] L. M. Krauss, S. Nasri and M. Trodden, Phys. Rev. D **67**, 085002 (2003) [arXiv:hep-ph/0210389].
 - [6] E. Ma, Phys. Rev. D **73**, 077301 (2006) [hep-ph/0601225].
 - [7] P. -H. Gu and U. Sarkar, Phys. Rev. D **77**, 105031 (2008) [arXiv:0712.2933 [hep-ph]].
 - [8] P. -H. Gu and U. Sarkar, Phys. Rev. D **78**, 073012 (2008) [arXiv:0807.0270 [hep-ph]].
 - [9] M. Aoki, S. Kanemura and O. Seto, Phys. Rev. Lett. **102**, 051805 (2009) [arXiv:0807.0361].
 - [10] M. Aoki, S. Kanemura, T. Shindou and K. Yagyu, JHEP **1007**, 084 (2010) [Erratum-ibid. **1011**, 049 (2010)] [arXiv:1005.5159 [hep-ph]].
 - [11] S. Kanemura, O. Seto and T. Shimomura, Phys. Rev. D **84**, 016004 (2011) [arXiv:1101.5713 [hep-ph]].
 - [12] M. Lindner, D. Schmidt and T. Schwetz, Phys. Lett. B **705**, 324 (2011) [arXiv:1105.4626 [hep-ph]].
 - [13] S. Kanemura, T. Nabeshima and H. Sugiyama, Phys. Lett. B **703**, 66 (2011) [arXiv:1106.2480 [hep-ph]].
 - [14] M. Aoki, J. Kubo, T. Okawa and H. Takano, Phys. Lett. B **707**, 107 (2012) [arXiv:1110.5403 [hep-ph]].
 - [15] S. Kanemura, T. Nabeshima and H. Sugiyama, Phys. Rev. D **85**, 033004 (2012) [arXiv:1111.0599 [hep-ph]].
 - [16] D. Schmidt, T. Schwetz and T. Toma, Phys. Rev. D **85**, 073009 (2012) [arXiv:1201.0906 [hep-ph]].
 - [17] S. Kanemura and H. Sugiyama, Phys. Rev. D **86**, 073006 (2012) [arXiv:1202.5231 [hep-ph]].

- [18] Y. Farzan and E. Ma, Phys. Rev. D **86**, 033007 (2012) [arXiv:1204.4890 [hep-ph]].
- [19] F. Bonnet, M. Hirsch, T. Ota and W. Winter, JHEP **1207**, 153 (2012) [arXiv:1204.5862 [hep-ph]].
- [20] K. Kumericki, I. Picek and B. Radovcic, JHEP **1207**, 039 (2012) [arXiv:1204.6597 [hep-ph]].
- [21] K. Kumericki, I. Picek and B. Radovcic, Phys. Rev. D **86**, 013006 (2012) [arXiv:1204.6599 [hep-ph]].
- [22] R. Bouchand and A. Merle, JHEP **1207**, 084 (2012) [arXiv:1205.0008 [hep-ph]].
- [23] E. Ma, Phys. Lett. B **717**, 235 (2012) [arXiv:1206.1812 [hep-ph]].
- [24] G. Gil, P. Chankowski and M. Krawczyk, Phys. Lett. B **717**, 396 (2012) [arXiv:1207.0084 [hep-ph]].
- [25] H. Okada and T. Toma, Phys. Rev. D **86**, 033011 (2012) arXiv:1207.0864 [hep-ph].
- [26] D. Hehn and A. Ibarra, Phys. Lett. B **718**, 988 (2013) [arXiv:1208.3162 [hep-ph]].
- [27] P. S. B. Dev and A. Pilaftsis, Phys. Rev. D **86**, 113001 (2012) [arXiv:1209.4051 [hep-ph]].
- [28] Y. Kajiyama, H. Okada and T. Toma, Eur. Phys. J. C **73**, 2381 (2013) [arXiv:1210.2305 [hep-ph]].
- [29] H. Okada, arXiv:1212.0492 [hep-ph].
- [30] M. Gustafsson, J. M. No and M. A. Rivera, Phys. Rev. Lett. **110**, 211802 (2013) arXiv:1212.4806 [hep-ph].
- [31] M. Aoki, J. Kubo and H. Takano, Phys. Rev. D **87**, no. 11, 116001 (2013) [arXiv:1302.3936 [hep-ph]].
- [32] Y. Kajiyama, H. Okada and K. Yagyu, Nucl. Phys. B **874**, 198 (2013) [arXiv:1303.3463 [hep-ph]].
- [33] Y. Kajiyama, H. Okada and T. Toma, Phys. Rev. D **88**, 015029 (2013) [arXiv:1303.7356].
- [34] S. Kanemura, T. Matsui and H. Sugiyama, Phys. Lett. B **727**, 151 (2013) [arXiv:1305.4521 [hep-ph]].
- [35] A. E. Carcamo Hernandez, I. d. M. Varzielas, S. G. Kovalenko, H. Päs and I. Schmidt, Phys. Rev. D **88**, 076014 (2013) [arXiv:1307.6499 [hep-ph]].
- [36] B. Dasgupta, E. Ma and K. Tsumura, Phys. Rev. D **89**, 041702 (2014) [arXiv:1308.4138 [hep-ph]].
- [37] A. E. Carcamo Hernandez, RMartinez and F. Ochoa, arXiv:1309.6567 [hep-ph].
- [38] K. L. McDonald, JHEP **1311**, 131 (2013) [arXiv:1310.0609 [hep-ph]].
- [39] S. Baek, H. Okada and T. Toma, JCAP **1406**, 027 (2014) [arXiv:1312.3761 [hep-ph]].
- [40] E. Ma, Phys. Lett. B **732**, 167 (2014) [arXiv:1401.3284 [hep-ph]].
- [41] A. Ahriche, S. Nasri and R. Soualah, Phys. Rev. D **89**, 095010 (2014) [arXiv:1403.5694 [hep-ph]].
- [42] H. Okada, arXiv:1404.0280 [hep-ph].
- [43] A. Ahriche, C. -S. Chen, K. L. McDonald and S. Nasri, arXiv:1404.2696 [hep-ph].
- [44] A. Ahriche, K. L. McDonald and S. Nasri, arXiv:1404.5917 [hep-ph].
- [45] C. -S. Chen, K. L. McDonald and S. Nasri, Phys. Lett. B **734**, 388 (2014) [arXiv:1404.6033 [hep-ph]].
- [46] S. Kanemura, T. Matsui and H. Sugiyama, Phys. Rev. D **90**, 013001 (2014) [arXiv:1405.1935 [hep-ph]].
- [47] M. Aoki and T. Toma, arXiv:1405.5870 [hep-ph].
- [48] M. Lindner, S. Schmidt and J. Smirnov, arXiv:1405.6204 [hep-ph].
- [49] Y. H. Ahn and H. Okada, Phys. Rev. D **85**, 073010 (2012) [arXiv:1201.4436 [hep-ph]].
- [50] E. Ma, A. Natale and A. Rashed, Int. J. Mod. Phys. A **27**, 1250134 (2012) [arXiv:1206.1570 [hep-ph]].
- [51] Y. Kajiyama, H. Okada and K. Yagyu, JHEP **10**, 196 (2013) arXiv:1307.0480 [hep-ph].
- [52] Y. Kajiyama, H. Okada and K. Yagyu, arXiv:1309.6234 [hep-ph].

- [53] E. Ma, Phys. Rev. Lett. **112**, 091801 (2014) [arXiv:1311.3213 [hep-ph]].
- [54] E. Ma and A. Natale, Phys. Lett. B **723**, 403 (2014) [arXiv:1403.6772 [hep-ph]].
- [55] H. Okada and K. Yagyu, Phys. Rev. D **89**, 053008 (2014) [arXiv:1311.4360 [hep-ph]].
- [56] S. Baek, H. Okada and T. Toma, Phys. Lett. B **732**, 85 (2014) [arXiv:1401.6921 [hep-ph]].
- [57] H. Okada and K. Yagyu, arXiv:1405.2368 [hep-ph].
- [58] D. Schmidt, T. Schwetz and H. Zhang, arXiv:1402.2251 [hep-ph].
- [59] H. N. Long and V. V. Vien, Int. J. Mod. Phys. A **29**, no. 13, 1450072 (2014) [arXiv:1405.1622 [hep-ph]].
- [60] V. Van Vien, H. N. Long and P. N. Thu, arXiv:1407.8286 [hep-ph].
- [61] J. Herrero-Garcia, M. Nebot, N. Rius and A. Santamaria, arXiv:1402.4491 [hep-ph].
- [62] F. Jegerlehner and A. Nyffeler, Phys. Rept. **477**, 1 (2009) [arXiv:0902.3360 [hep-ph]].
- [63] M. Benayoun, P. David, L. Delbuono and F. Jegerlehner, Eur. Phys. J. C **72**, 1848 (2012) [arXiv:1106.1315 [hep-ph]].
- [64] T. P. Cheng and L. -F. Li, Phys. Rev. D **22**, 2860 (1980).
- [65] J. Schechter and J. W. F. Valle, Phys. Rev. D **22**, 2227 (1980).
- [66] G. Lazarides, Q. Shafi and C. Wetterich, Nucl. Phys. B **181**, 287 (1981).
- [67] R. N. Mohapatra and G. Senjanovic, Phys. Rev. D **23**, 165 (1981).
- [68] M. Magg and C. Wetterich, Phys. Lett. B **94**, 61 (1980).
- [69] P. A. R. Ade *et al.* [Planck Collaboration], arXiv:1303.5076 [astro-ph.CO].
- [70] T. Hambye, F. -S. Ling, L. Lopez Honorez and J. Rocher, JHEP **0907**, 090 (2009) [Erratum-ibid. **1005**, 066 (2010)] [arXiv:0903.4010 [hep-ph]].
- [71] L. Lopez Honorez, E. Nezri, J. F. Oliver and M. H. G. Tytgat, JCAP **0702**, 028 (2007) [hep-ph/0612275].
- [72] D. S. Akerib *et al.* [LUX Collaboration], arXiv:1310.8214 [astro-ph.CO].
- [73] D. Tucker-Smith and N. Weiner, Phys. Rev. D **64**, 043502 (2001) [hep-ph/0101138].
- [74] M. E. Peskin and T. Takeuchi, Phys. Rev. Lett. **65**, 964 (1990); M. E. Peskin and T. Takeuchi, Phys. Rev. D **46**, 381 (1992).
- [75] M. Baak, M. Goebel, J. Haller, A. Hoecker, D. Kennedy, R. Kogler, K. Moenig and M. Schott *et al.*, Eur. Phys. J. C **72**, 2205 (2012) [arXiv:1209.2716 [hep-ph]].
- [76] D. Aristizabal Sierra and M. Hirsch, JHEP **0612**, 052 (2006) [hep-ph/0609307].
- [77] Z. Maki, M. Nakagawa and S. Sakata, Prog. Theor. Phys. **28**, 870 (1962).
- [78] D. V. Forero, M. Tortola and J. W. F. Valle, arXiv:1405.7540 [hep-ph].
- [79] F. Beutler *et al.* [BOSS Collaboration], arXiv:1403.4599 [astro-ph.CO].
- [80] G. W. Bennett *et al.* [Muon G-2 Collaboration], Phys. Rev. D **73**, 072003 (2006) [hep-ex/0602035].
- [81] [ATLAS Collaboration], Report No. ATLAS-CONF-2013-049.
- [82] A. Pukhov, [hep-ph/0412191].
- [83] K. S. Babu and C. Macesanu, Phys. Rev. D **67**, 073010 (2003) [hep-ph/0212058].
- [84] M. Nebot, J. F. Oliver, D. Palao and A. Santamaria, Phys. Rev. D **77**, 093013 (2008) [arXiv:0711.0483]

- [hep-ph]].
- [85] P. Fileviez Perez, T. Han, G. -y. Huang, T. Li and K. Wang, Phys. Rev. D **78**, 015018 (2008) [arXiv:0805.3536 [hep-ph]].
 - [86] C. -W. Chiang, T. Nomura and K. Tsumura, Phys. Rev. D **85**, 095023 (2012) [arXiv:1202.2014 [hep-ph]].
 - [87] S. Kanemura, K. Yagyu and H. Yokoya, Phys. Lett. B **726**, 316 (2013) [arXiv:1305.2383 [hep-ph]].
 - [88] Z. Kang, J. Li, T. Li, Y. Liu and G. -Z. Ning, arXiv:1404.5207 [hep-ph].
 - [89] S. Kanemura, M. Kikuchi, K. Yagyu and H. Yokoya, arXiv:1407.6547 [hep-ph].